

Chapter 1

GENERAL INTRODUCTION

1.1 New Carbon Materials

The carbon is one of the popular materials and exists in quantity on the earth with polymorphous forms. The carbon is capable of constructing various materials with other elements. A wide field of the organic chemistry shows a variety of the carbon related materials. This variety of the carbon materials is due to the capability of carbon atoms to take various coordination numbers from two to four. The $2s$ and $2p$ orbitals of the carbon can hybridize to form covalent bonds with other atoms. The carbon atom has three kinds of the hybridizations, *i.e.* sp , sp^2 and sp^3 hybridizations. These sp , sp^2 and sp^3 hybridizations correspond to the coordination numbers of 2, 3 and 4, respectively. For the case of simple hydrocarbon molecules, the carbon atoms construct a linear molecule of acetylene (sp -carbon), a planar molecule of ethylene (sp^2 -carbon) and a 3-dimensional molecule of methane (sp^3 -carbon). On the other hand, for the carbon crystal, the sp^2 -carbon construct the 2-dimensional graphite honeycomb network and the sp^3 carbon construct the 3-dimensional diamond network as shown in Fig. 1.1. It had been considered for a long time that the networks

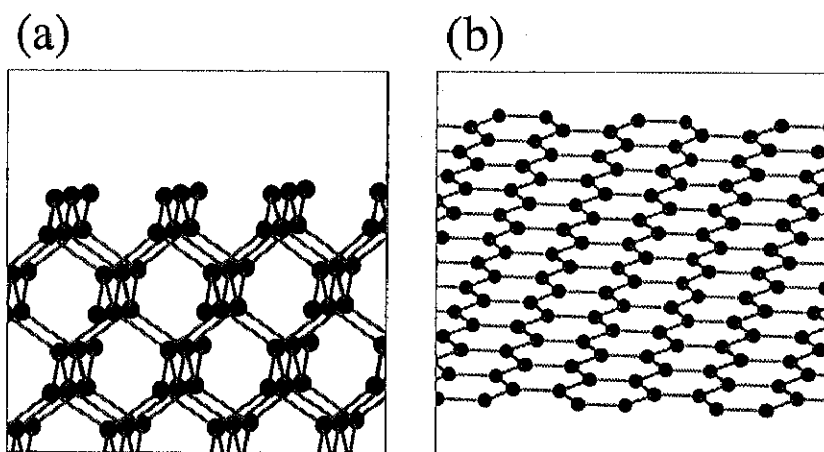


Figure 1.1: The networks of the carbon crystals are depicted. (a) Diamond: This 3-dimensional network is constructed only by the sp^3 carbons. (a) Graphite: This 2-dimensional network is constructed only by the sp^2 carbons.

constructed only by the carbon atoms are the graphite and the diamond.

The discovery of a new carbon network by Kroto and Smalley was a breakthrough in the carbon related material science; they discovered the closed cage structures consisting only of the sp^2 carbons C_{60} [1]. These closed cage molecules of the sp^2 carbon are termed as “fullerenes” (or “Buckminsterfullerenes”). In addition to the C_{60} , other closed networks C_{70} and C_{84} and so on, have been discovered. For example, the structures of the C_{60} , C_{70} and C_{84} are depicted in Fig. 1.2. All the closed networks of the sp^2 carbon have 12 pentagons. It is impossible to construct the closed

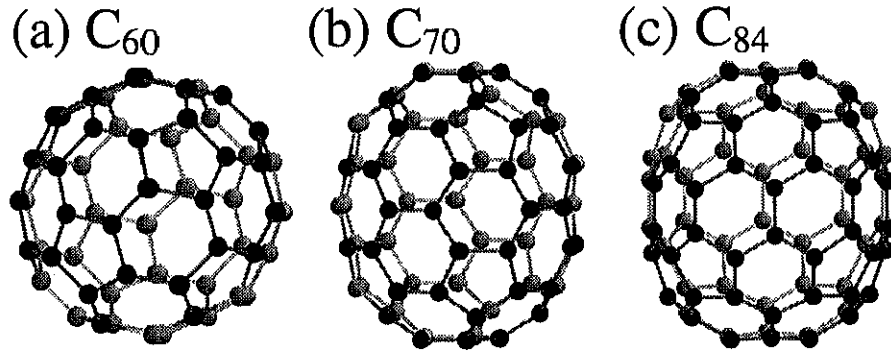


Figure 1.2: Three dimensional views of the close cage structures of the fullerenes. Atoms on the far side in these figures are indicated by the lighter spheres for clarity. We depict the C_{60} (a), C_{70} (b) and C_{84} (c), for example clusters of the fullerene family. These clusters are synthesized with relatively high yields.

network only from the hexagons. The sp^2 carbon network obtains the curvature by introducing pentagons. When the 12 pentagons are introduced into the sp^2 carbon network, the network is closed completely. This number of pentagons required to close the sp^2 network is determined by the geometry. (This number of pentagon is derived from the *Euler's theorem*.) Furthermore, it is well known that the adjacent pentagons pair is usually avoided in the synthesized fullerenes (*isolated pentagon rule IPR*)[2]. It is also known that the C_{60} is the smallest fullerene that satisfies the IPR. The fullerenes which are smaller than the C_{60} cannot satisfy the IPR. The next smallest fullerene that satisfies the IPR is the C_{70} . The researches for these fullerenes advanced greatly since Krätschmer *et al.* developed a simple method to synthesize the fullerenes in 1990 [3]. They have synthesized the fullerenes with high yield by evaporating the graphite electrodes. It has been reported that the fullerenes can be also synthesized by the laser ablation [4] and the arc discharge [5] methods.

1.2 Carbon Nanotubes

Within the carbon networks, the diamond and the graphite construct the 3-dimensional and the 2-dimensional networks, respectively. The closed network of the fullerenes corresponds to the 0-dimensional network of the sp^2 carbon. In addition to the fullerenes, new structures which correspond to 1-dimensional networks of the sp^2 carbons were discovered by Iijima in 1991; the

carbon nanotubes (NTs) [6].

The carbon nanotubes were discovered in deposits on the negative electrode of the arc discharge apparatus. The carbon nanotube is formed by rolling up the single graphite sheet into the tubule structure with nanoscale radius. At the first discovery, the carbon nanotubes consisted of several coaxial tubules. These carbon nanotubes are termed as the “multi-wall carbon nanotubes” (MWNTs). On the other hand, the carbon nanotube which consists of a single layer of the graphite is termed as the “single-wall carbon nanotubes” (SWNTs). The schematic views of these structures of two kinds of nanotubes are shown in Fig. 1.3. The interlayer distance in the MWNT is always

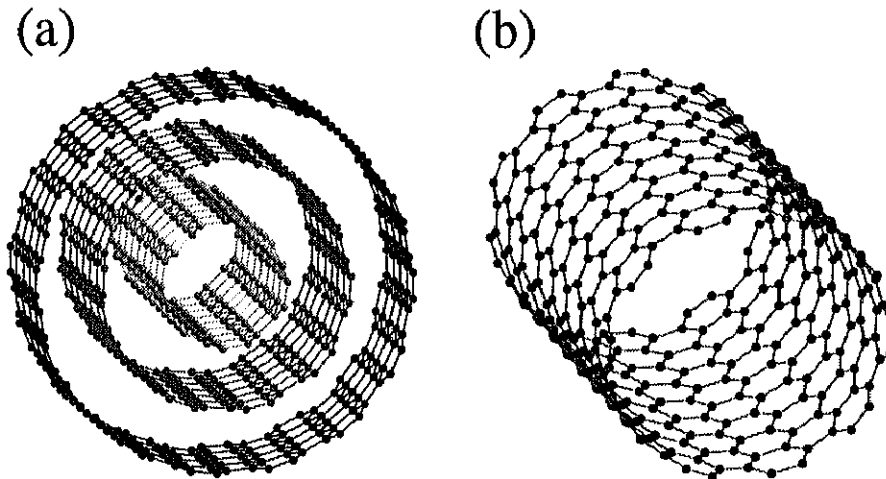


Figure 1.3: Three dimensional view of the typical structures of the multi-wall carbon nanotube (MWNT) and the single-wall carbon nanotube (SWNT) are depicted. (a) The MWNT (3-wall NT): This MWNT consists of 3 coaxial NTs, *i.e.* the (5,5)-tube (centre tube; light gray spheres), the (10,10)-tube (middle tube; dark-gray spheres) and the (15,15)-tube (outer tube; black spheres). The interlayer distance of the MWNT is always $\sim 3.4 \text{ \AA}$ which is similar to the interlayer distance of the graphite. The radii of the (5,5)-tube, the (10,10)-tube and the (15,15)-tube are 3.4 \AA , 6.8 \AA and 10.2 \AA , respectively. (b) The SWNT: The (10,10)-tube is depicted for example.

$\sim 3.4 \text{ \AA}$ which is almost same as the interlayer distance of the graphite.

Since the carbon nanotube was discovered, a large amount of both the theoretical and experimental efforts has been performed. This is due to fascinating electronic [7, 8, 9] and mechanical [10, 11, 12, 13, 14, 15, 16] properties of the NTs. On the other hand, the method of the NT synthesis is now being established: The NT is synthesized by three sorts of methods, that is, the laser ablation [17, 18], the arc discharge [19] and the chemical vapor deposition (CVD) [20, 21]. It has been already known that catalysts of the transition metals are required for the synthesis of the SWNTs. The typical transition metals used as the catalysts are the Fe [22], Co [23] and Ni [24]. The other transition metals such as Y, La, Ce, Pt, Rh and Pd, are also used as the catalysts to synthesize the SWNTs. Furthermore, the mixtures of the transition metals, that is, Fe+Ni [25] and Ni+Y [26] for example, are used to increase the yield of the SWNT. Thess *et al.* have achieved the high yield synthesis of SWNTs by the laser ablation method in 1996 [18]. Recently, a number

of efforts to increase the yields of the NT synthesis and to control the radius of the NT by changing the catalyst metals or growth temperature [25, 26, 27, 28, 29, 30] are being performed.

1.3 Properties and Applications of Carbon Nanotubes

It has been considered that the small graphite sheet has tendency to obtain curvature because of the dangling bonds (DBs) on the edge atom. The number of the DBs decreases by introducing the pentagon into the small graphite sheet without changing the total number of the carbon atoms. The fullerene is the completely closed cage structure without DBs. On the other hand, when the graphite sheet is rolled up into the tubule structure, the number of DB is also reduced without pentagons. Although the strain is induced by the curvature for both case of the fullerene and the nanotube, the elimination of the DBs compensates the energy loss by the strain. In the case of the open edge nanotube, the DBs exist on the edge atoms. Hence, the almost all synthesized nanotubes are closed by the fullerene hemisphere structures. (This fullerene hemisphere terminating the nanotube edge is termed as the “cap structure”.)

The way of rolling up the graphite sheet determines the geometrical structure of the nanotube (radius and chirality). In other words, the geometrical structure of the carbon nanotubes is uniquely specified by the chiral vector \mathbf{C} which connects two crystallographically equivalent points O_1 and O_2 in the carbon nanotube as shown in Fig. 1.4 (a). The chiral vector \mathbf{C} is defined in the graphite sheet as

$$\mathbf{C} = m\mathbf{a}_1 + n\mathbf{a}_2 \quad (1.1)$$

where $\mathbf{a}_1 = (a, 0)$ and $\mathbf{a}_2 = (\frac{a}{2}, \frac{\sqrt{3}}{2}a)$ are the unit vectors of the graphite sheet ($a=2.46 \text{ \AA}$ is the lattice constant of the graphite) and m and n are integers. The chiral angle θ is indicated in Fig. 1.4(a). The carbon nanotube is denoted by the pair of integers (m, n) (The tube index. The notation of the tube indexes by Saito *et al.* [8] is adopted in this thesis.). The tube indexes are shown in Fig. 1.4(b). The (m, n) -tube is formed by rolling up the graphite sheet so as to superpose the hexagon at the origin upon the hexagon at the (m, n) site. The radius R and the chiral angle θ of the (m, n) -tube are represented by m and n as,

$$R = \frac{|\mathbf{C}|}{2\pi} = \frac{\sqrt{m^2 + mn + n^2}}{2\pi} a, \quad (1.2)$$

$$\theta = \tan^{-1} \left(\frac{\sqrt{3}n}{2m + n} \right) \quad (|\theta| \leq 30^\circ). \quad (1.3)$$

The range of the chiral angle is due to the symmetry of the graphite sheet. The two typical nanotubes are formed when $m = n$ ($\theta = 30^\circ$) and $n = 0$ ($\theta = 0^\circ$), that is armchair tube and zigzag tube, respectively. These nanotubes are achiral tubes. We depict these achiral nanotubes, that is, the (5,5)-tube for the armchair type and the (9,0)-tube for the zigzag type, with the cap structures (hemispheres of the fullerene) in Fig. 1.5. One edge of each nanotube (top edge) is closed by the cap structure, and the other edge (bottom edge) is left open. As mentioned above, the DBs are eliminated by the closure of the nanotube edge with fullerene hemisphere. In the case

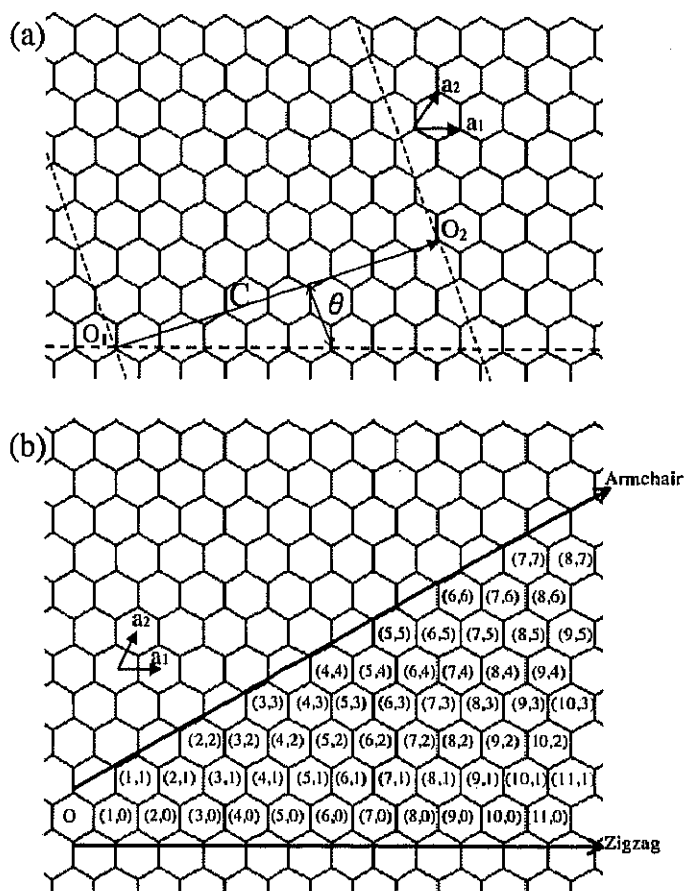


Figure 1.4: (a) The single graphite sheet is depicted. The carbon nanotube is constructed in order to connect together the points O_1 and O_2 . The vector \mathbf{C} is the chiral vector represented by the linear combination of the unit vectors of the graphite \mathbf{a}_1 and \mathbf{a}_2 . (See text.) The chiral angle is indicated by θ . The two dotted lines perpendicular to the chiral vector \mathbf{C} correspond to the cylinder joint of the carbon nanotube. (b) The tube indexes (m, n) are indicated. The (m, n) -tube is formed in order to superpose the hexagon at the origin O upon the hexagon at the (m, n) site. When $m = n$ ($\theta = 30^\circ$), the achiral armchair tube is formed. When $n = 0$ ($\theta = 0^\circ$), the achiral zigzag tube is formed. The other tubes are termed as chiral tubes.

of the (5,5)-tube and the (9,0)-tube, the hemisphere of the C_{60} can fit both edges of the (5,5)- and (9,0)-tubes. (The hemisphere that fit the (5,5)-tube edge (the (9,0)-tube edge) possesses the pentagon (hexagon) pole at the top.)

It has been reported that the electronic structures of carbon nanotube can be predicted from that of the graphite [7, 8]: In the level of Hückel tight-binding model, the electronic state of the carbon nanotube is that of the single graphite sheet with the periodic boundary condition imposed along the chiral vector. As a result, it is concluded that the (m, n) -tubes which satisfy the condition of $m - n = 3q$ (q is an integer) become metallic tubes and the other nanotubes become semi-conductive tubes [7, 8]. It is surprising that the nanotubes can become either the metal or the semi-conductor only by changing its geometrical structure. Only the carbon nanotube possesses this fascinating character. These discussions neglect the effect of the curvature of the nanotube.

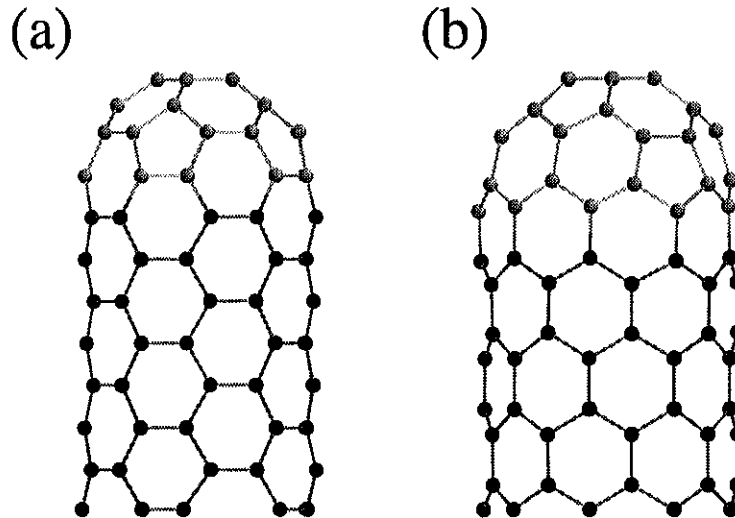


Figure 1.5: Side views of the two typical single-wall nanotubes with hemispheres of the fullerene C_{60} are depicted. For clarity, the atoms of the cap structures are indicated by the lighter spheres. (a) The armchair type nanotube: This nanotube is the (5,5)-tube. The cap structure is the C_{60} hemisphere with the pentagon on the top. (b) The zigzag type nanotube: This nanotube is the (9,0)-tube. The cap structure is the C_{60} hemisphere with the hexagon on the top.

However, this effect turns to be negligible in the large radius nanotube.

Recently, scanning tunneling microscope (STM) and scanning tunneling spectroscopy (STS) observations have achieved the identification of both the geometric and electronic structures [31, 32, 33, 34]. These observations have revealed the relationship between the geometrical and electronic structures originally predicted by the theory [7, 8]. In addition to the electronic properties, fascinating mechanical properties have been reported [10, 11, 12, 13, 14, 15, 16]. The nanotube is a light and very flexible material. These remarkable properties imply that the carbon nanotubes can be used as the strong carbon fibers.

Because of these fascinating properties of the carbon nanotube, various scientific and industrial applications are already proposed: the tip of the STM and the atomic force microscope (AFM) [35, 36, 37], the nanoscale electronic device [38, 39, 40, 41], the electrode of the lithium-ion battery [42], the storage of the hydrogen molecules [43] and the emitter of the field emission display [44] and so on. For the STM tip, it is already known that the nanotube possesses the properties required for the STM tip: atomic-scale sharpness, conductive, chemically inactive and well-known atomic structure. The flexibility of the nanotube is also available for the tip of the STM and AFM. For the electronic devices, it has been shown that the nanotube can work as the transistor [40, 41] or capacitor [39]. The nanotube also becomes the quantum wire. On the other hand, it has been reported that the various atoms and molecules can be doped in the carbon nanotube bundles or inside the carbon nanotubes (doped nanotubes) [45, 46, 47]. These doped nanotubes are analogies of the graphite intercalation compounds [48] and the doped solid fullerenes [49, 50, 51, 52]. The hydrogen doped carbon nanotubes are expected to be applied as a fuel cell of an electronic vehicle [43]. When the

lithium is doped into the carbon nanotube, this doped nanotube can be used as the electrode of the secondary lithium-ion battery [42]. However, these applications are still in the experimental stage. The establishment of the mass production of the carbon nanotubes is required to develop the applications of the nanotubes further and to commercialize the carbon nanotubes.

1.4 Growth Mechanisms of Carbon Nanotubes.

Although the carbon nanotube has wide range of application fields, the growth mechanisms of the carbon nanotubes are not confirmed. It is imperative to identify the growth mechanisms in order to develop a way of the mass production of the carbon nanotube and to control its shape (radius and chirality). There has been a number of efforts to reveal the atomic scale processes in the carbon nanotube growth phenomena. In the theoretical side, various growth models have been investigated. These growth models can be roughly classified into two types, that is, the open edge growth model and the closed edge growth model. Schematic diagrams illustrating these two growth models of the NTs are shown in Fig. 1.6. In the open edge growth model, it is considered

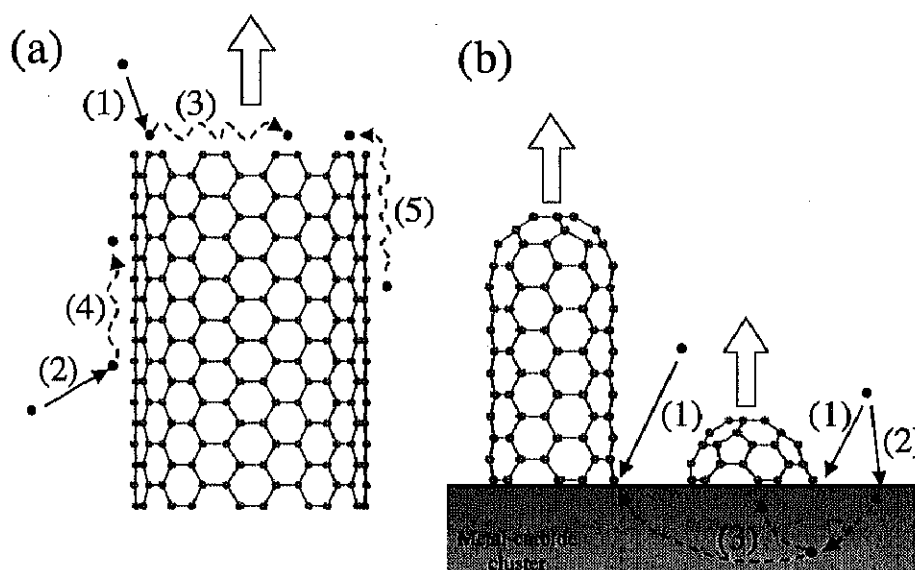


Figure 1.6: Diagrams of the open edge growth model (a) and the closed edge growth model (b). (a) The NT grows with the open edge. The carbon adatom is adsorbed on the NT edge (1) and the NT wall (2). These adatoms diffuse on the edge (3) or the wall (4). The adatom on the edge is expected to be incorporated into the NT honeycomb lattice. In addition, it is also expected that the adatom on the wall diffusing toward the edge is also incorporated at the open edge (5). Consequently, the NT grows successively. (b) The NT grows with the closed edge on the metal-carbide cluster. It is considered that the carbon atoms are not easily incorporated into the NT lattice at the closed edge. Therefore, the carbon atoms are adsorbed at the root of the NT (1). It is also proposed that the carbon atoms are absorbed into the metal-carbide cluster (2), followed by that the carbon atoms in the cluster diffuse toward the root of the NT (3). These carbon atoms are incorporated into the NT honeycomb lattice at the root of the NT.

that the edge of the nanotube is kept open during growth. The nanotube grows by incorporation

of carbon atoms into the honeycomb lattice of the nanotube at the open edge. (This growth model is analogy of the layer-by-layer growth of the usual material.) When the open edge is closed by a certain mechanism, the growth is stopped. Within this model, the mechanisms to stabilize the open edge and the behavior of carbon or other catalyst metal atoms have been investigated. On the other hand, in the closed edge growth model, it is assumed that the nanotubes grow from the metal-carbide cluster. The top edge is closed by the cap structure during growth. It is considered that the metal-carbide cluster supplies the carbon atoms to the roots of the nanotubes and then the nanotube grow from the metal-carbide cluster. (Therefore, this growth model is also termed as the “root growth model”. See Fig. 1.6 (b).)

Along this line, various models of the SWNT and MWNT have been already proposed: the open edge growth model [53, 54, 55, 56], the root growth model [57], the catalytic growth model [58, 59, 60], the lip-lip interaction model [61, 62, 63, 64], the step flow growth model [65] and the cap formation growth model (This “cap” indicates also the fullerene hemisphere) [66]. In the open edge growth model, the strength of the electric field at the nanotube edge which may stabilize the dangling bonds on the edge is estimated and behaviors of adatoms on the nanotube edge is simulated by the classical molecular dynamics (MD) [53, 54]. The energies of the several configurations of the pentagons, hexagons and heptagons are also calculated [54]. In the root growth model, the SWNT is assumed to grow from the metal-carbide cluster. Maiti *et al.* simulated incorporation of carbon atoms into the hexagon network of nanotube at the root of the nanotube with the molecular dynamics simulations [57]. In the catalytic growth model, a role of the transition metal catalyst which is speculated to be necessary for the SWNT growth is proposed: Lee *et al.* have shown that an activation barrier for edge diffusion of a Ni atom is less than that of the C atom [59]: The Ni atom diffusing on the nanotube edge assists in annealing out defects such as a pentagon which is responsible for the tube closure. In the lip-lip interaction model, two aspects are discussed. Kwon *et al.* have calculated total energies of several edges of MWNTs with adatoms using the cluster code DMol [67] and the parametrized linear combination of atomic orbitals method. They have shown that the edges of the MWNTs are stabilized against tube closure by interactions between the inner and outer tubes (the lip-lip interaction) [62]. The lip-lip interaction in this case is mediated by the adatoms placed between the inner and outer tube. On the other hand, Nardelli *et al.* have concluded from the MD simulation that the lip-lip interaction does not stabilize open edges of the MWNT, but rather facilitates the tube closure [63, 64]: The lip-lip interaction induces transfer of adatoms from the outer tube edge to the inner tube edge, followed by that the several pentagons which induce the tube closure are formed on the edge of the inner tube. This results in the closure of the inner tube. In the step flow growth model, the length and growth rate of the MWNT are estimated [65]. In the cap formation growth model, the energy gain of the cap formation on the nanotube open edge is calculated for the armchair and zigzag nanotube [66]. It is found that the energy gain upon cap formation in the zigzag nanotube is larger than in the armchair nanotube. Accordingly, the open edge of the zigzag nanotube tends to be closed by the

cap formation compared with the armchair nanotube.

These efforts have certainly clarified several aspects of growth of carbon nanotubes. In clarification of crystal surface growth, however, identification of surface structures on which the crystal grows and determination of adatom adsorption sites at initial stages of the growth are usually investigated [68]. As to this aspect, our understanding about the carbon nanotubes is less satisfactory. It is imperative to identify microscopic edge structures of nanotubes, adsorption sites of carbon adatoms near the stable edges and behaviors of the carbon adatoms on the edge.

1.5 The Organization of this Thesis

In this thesis, being concentrated on the open edge growth of the single wall carbon nanotube, the energetics of the finite-length nanotubes with edges and the atomic processes near the nanotube edge are presented. The density functional calculations and the tight-binding model calculations are performed. Details of the methods of calculations are given in each chapter. This thesis is organized as follows.

In chapter 2, all calculations are performed by the transferable tight-binding (TTB) model. The large radius NTs in which the density functional calculation is formidable are investigated by the TTB model. The energetics and kinetics of the NT growth are discussed within the TTB calculations. We obtain in this chapter the total energies of finite-length carbon nanotubes as functions of a number of atoms N . It is found that the most stable finite-length nanotube at a fixed number of N is always the armchair type. Furthermore, the radius of the most stable nanotube increases with increasing N .

In chapter 3, more accurate calculations by the density functional theory (DFT) with the local density approximation (LDA) are performed. The edge structures and the energies of the polygonal network, such as the pentagon, hexagon and heptagon networks, on the NT edge are calculated. In this chapter, we concentrate on the behavior of the carbon adatoms on the edge of the NT. The diffusion processes of the carbon adatoms are discussed in detail. During the open edge growth, several pentagons are likely to be formed on the edge by the adatoms adsorption. It is well known that the pentagon in the NT honeycomb lattice introduces the positive curvature [69] and promotes the tube closure. The polygonal defects such as the pentagon on the NT edge must be annealed out to maintain the open edge growth. Thus, we also investigate annealing out of the polygonal defects on the NT edge. For annealing out of the polygonal defects, incorporation of the adatom on the nanotube edge or the nanotube wall into the polygonal defects is discussed. By calculations of the activation energies of incorporation, it is found that the adatom on the nanotube wall is incorporated into the polygonal defects more easily than the adatom on the nanotube edge.

In chapter 4, atomic step structures on the NT edge are investigated. During the open edge growth of the NT, flatness along the NT edge is not always guaranteed. Atomic steps as in material surfaces are likely to exist. Importance of atomic steps in growth phenomena is widely recognized, for instance, in semiconductor epitaxial growth [70, 71]. Toward understanding of roles

of steps in the NT growth, we here identify structures and formation energies of atomic steps at edges of NTs. Within the TTB model, we considered a single- and double-row step each for the armchair nanotube edge and zigzag nanotube edge. The step formation energies are calculated for various radii. On the other hand, the LDA calculations are performed for the (8,8)-tube. The stable or metastable adsorption sites near the step structure are explored by the LDA calculation. It is found that the site just below the step is a sink for the edge adatoms, indicating that the adatoms on the edge are likely to be adsorbed on this site. The flattening of steps is a general trend on the armchair edge.

In chapter 5, We summarize the results of this thesis.